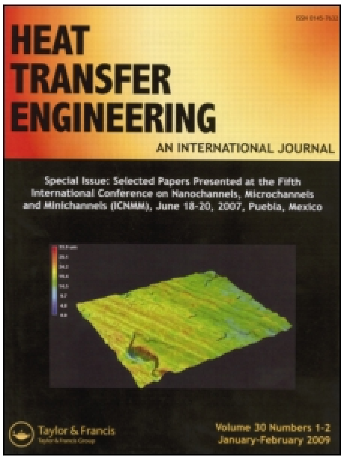

Heat Transfer Engineering
Publication details, including instructions for authors and subscription information:
http://www.informaworld.com/smpp/title~content=t713723051

A Nonlinear Solution of Inverse Heat Conduction Problem for Obtaining the Inner Heat Transfer Coefficient

Jinliang Xu[a]; Tingkuan Chen[b]
[a] Institute of Nuclear Energy Technology, Tsinghua University, Beijing, People's Republic of China [b] National Laboratory on Multiphase Flow in Power Engineering, Xi'an Jiaotong University, Xian, People's Republic of China

A Nonlinear Solution of Inverse Heat Conduction Problem for Obtaining the Inner Heat Transfer Coefficient

JINLIANG XU

Institute of Nuclear Energy Technology, Tsinghua University, Beijing, People's Republic of China

TINGKUAN CHEN

National Laboratory on Multiphase Flow in Power Engineering, Xi'an Jiaotong University, Xian, People's Republic of China

When steam–water two-phase mixtures flow in inclined or horizontal tubes that are heated by alternating current, the circular angle-dependent temperatures on the outer radius imply that the inner heat transfer coefficients also vary with circular angle. The inner heat transfer coefficients are difficult to measure directly, but may be determined with the aid of inverse heat conduction theory. The direct model calculates the temperature field inside a half-pipe. This is subjected to a given heat transfer coefficient angular profile on its inner radius. The inverse heat conduction model calculates the temperature field under the conditions of the measured discrete temperatures and the heat-insulated boundary on the outer radius. Variation of the cylinder heat conductivity and specific resistance versus temperatures are considered in both models. The prediction accuracy is analyzed with a numerical test. The inverse heat conduction problem solution is verified as a useful tool for obtaining the inner heat transfer coefficient.

Measuring the local heat transfer coefficient h by the direct method between a point M on a wall and a fluid at temperature T_f poses a difficult problem: One has to measure at the same spot both a wall temperature T and a heat flux Q, which passes through a section of area ΔS centered at M as shown in Figure 1.

When two-phase mixture flows in a vertical tube that is uniformly heated by electrical resistance or boiler flame, the inner heat transfer coefficients can be easily obtained by measuring the uniform heat flux and wall temperature on the outer tube surface. (The temperature on the inner tube wall surface can be easily predicted by the one-dimensional heat conduction equation.) However, it is difficult to do this for two-phase mixtures flowing in inclined or horizontal tubes. The natural convection at the cross section may affect the inner heat transfer coefficient distribution along circular angles. From our experiments performed in the high-pressure convective test loop of Xi'an Jiaotong University, we know that at certain conditions, the temperature at the top point on the outer radius begins to rise, while the

Received 13 September 1996; accepted 8 July 1997.

Address correspondence to Dr. Jinliang Xu, Institute of Nuclear Energy Technology, Tsinghua University, Beijing, 100084, People's Republic of China. E-mail: xsr.ine@mail.tsinghua.edu.cn

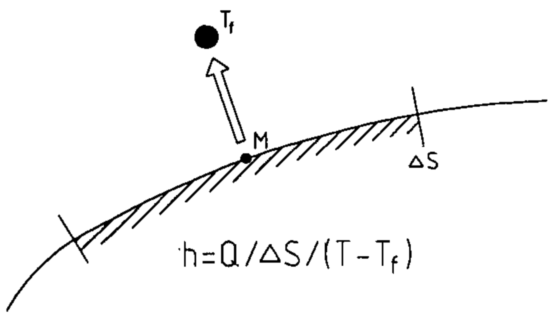

Figure 1 Direct measurement of local heat transfer coefficient.

temperatures at lower points keep the normal values, from these we infer that heat transfer deterioration occurs in the region neighboring the top point. In order to obtain insight into the nonuniform heat transfer coefficient distribution, the two-dimensional wall temperature field should be solved with the aid of inverse heat conduction theory.

One inverse problem in heat conduction theory consists of estimating the temperature and flux on the surface of a conduction solid from temperature measurements made within or at a secondary surface of the solid [1]. This problem is encountered frequently in situations where it is impossible to monitor the desired quantities directly. Typical examples are the estimation of surface heat transfer from measurements made within the skin of a reentry vehicle, and the prediction of temperature and heat flux from calorimeter-type instrumentation. Many researchers have examined the inverse problem, and a number of approaches have been offered. A great many of investigations concerned the one-dimensional transient or steady-state problem. Hills and Hensel [2] considered the one-dimensional nonlinear problem of heat conduction using a noniterative space-marching finite-difference algorithm. Flach and Ozisik [3] presented an adaptive sequential method to solve the inverse heat conduction problem. Kurpisz [4], and Maillet and Degiovanni [5], are authors who contributed to the multidimensional inverse heat conduction problem. Maillet and Degiovanni [5] used an analytical or a boundary-element technique to treat the steady-state two-dimensional problem. Recently, Keanini and Desai [6] developed an inverse finite-element method for predicting multidimensional phase-change boundaries and nonlinear solid-phase heat transfer.

The direct model is first applied, using the finite-difference numerical solution. Then the nonlinear inverse heat conduction problem is solved when the outer wall surface is well insulated, and the discrete temperatures on the outer radius are obtained. A numerical test is performed to discuss the test error of temperatures on the inner heat transfer coefficient; example results are also provided using real experimental data from the test facility of the authors' laboratory.

DIRECT HEAT CONDUCTION PROBLEM SOLUTION (DHCS)

In the boiling two-phase heat transfer experiment, the electrical resistance is usually used to heat the mixture inside the tube directly. As shown in Figure 2, across the distance L, with inner diameter D_i, the voltage applied in the tube is V, the current is I. If we ignore the heat release from the outer surface, the average heat flux on the inner radius is $\bar{q} = VI/(\pi D_i L)$. In order to perform the numerical test on the temperature error on the inner heat transfer coefficient in the inverse heat conduction problem, we start the process of direct heat conduction problem solution. At cross section A (Figure 2), one-half of the tube geometry is considered due to the geometry symmetry. In the present study, the control-volume heat balance method and homogeneous grids are used; the control-volume method and the diffusive problem solution are classical and can be found in [7].

The outer surface is assumed to be well heat insulated, the inner surface is assumed to acquire a known heat transfer coefficient distribution. The thermal conductivity K and specific electrical resistance ρ should be considered as functions of local temperature.

The steady-state heat conduction equation can be written as

$$\frac{1}{r}\frac{\partial}{\partial r}\left(rK\frac{\partial T}{\partial r}\right) + \frac{1}{r}\frac{\partial}{\partial \theta}\left(\frac{K}{r}\frac{\partial T}{\partial \theta}\right) + S = 0 \qquad (1)$$

where S is the heat source term. For internal nodes, the relationship between $T(I, J)$ and the four neighboring node temperatures can be obtained by integrating Eq. (1) in control volume $P(I, J)$; see Figure 3.

$$a_P T_P = a_E T_E + a_W T_W + a_N T_N + a_S T_S + b(I, J) \qquad (2)$$

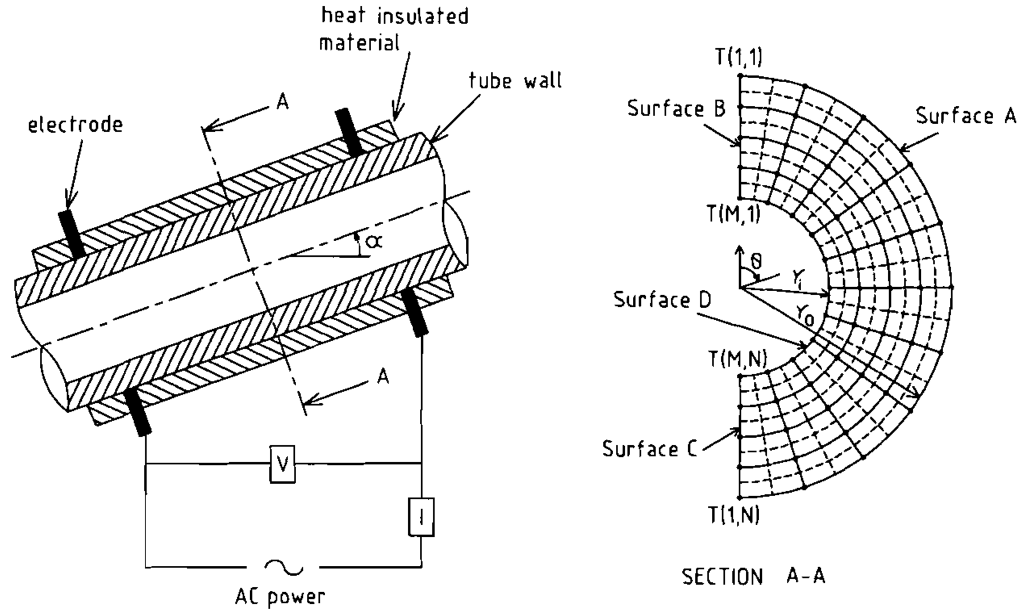

Figure 2 Inclined tube arrangement.

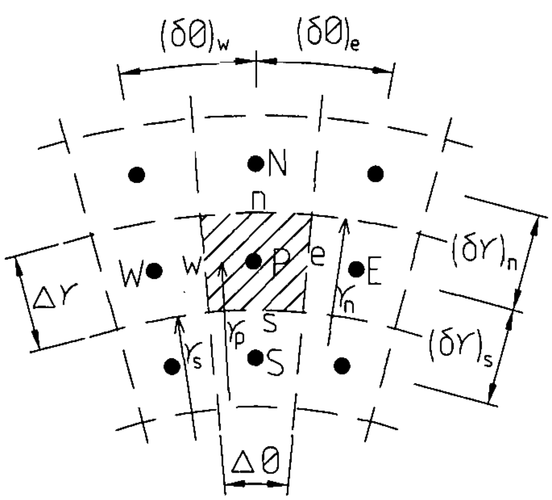

Figure 3 Two-dimensional grid system.

where

$$a_E = \frac{\Delta r}{r_e(\delta\theta)_e/K_e} \qquad a_W = \frac{\Delta r}{r_w(\delta\theta)_w/K_w}$$

$$a_N = \frac{r_n\,\Delta\theta}{(\delta r)_n/K_n} \qquad a_s = \frac{r_s\,\Delta\theta}{(\delta r)_s/K_s}$$

$$b = S\,\Delta V$$

In the present study, $(\delta\theta)_e = (\delta\theta)_W = \Delta\theta, (\delta r)_n = (\delta r)_s = \Delta r$, $a_P = a_E + a_W + a_N + a_S$, where ΔV is the volume of $P(I, J)$.

In Eq. (2), $b(I, J)$ represents the heat produced in control volume $P(I, J)$ per unit length; it will be specified in detail in a later section. Equation (2) is correct for the internal nodes, that is, $2 \le I \le M - 1, 2 \le J \le N - 1$.

BOUNDARY CONDITIONS

As shown in Figure 2, surface A is heat insulated; surface B and surface C are also heat insulated due to the geometry symmetry.

Based on the method of control-volume heat balance, the discrete temperatures $[T(1, J), 2 \le J \le N - 1]$ on surface A can be written as

$$a_P T(1, J) = a_E T(1, J + 1) + a_W T(1, J - 1) + a_S T(2, J) + b(1, J) \tag{3}$$

where

$$a_E = \frac{\Delta r}{2r_o\,\Delta\theta/K_e} \qquad a_W = \frac{\Delta r}{2r_o\,\Delta\theta/K_w}$$

$$a_S = \frac{r_s\,\Delta\theta}{\Delta r/K_s} \qquad a_P = a_E + a_W + a_S$$

$$r_s = r_o - 0.5\,\Delta r$$

For $T(1,1)$ and $T(1,N)$, we have

$$(a_E + a_S)T(1,1) = a_E T(1,2) + a_S T(2,1) + b(1,1) \quad (4)$$

$$a_E = \frac{\Delta r}{2r_o\,\Delta\theta/K_e} \qquad a_S = \frac{r_s\,\Delta\theta}{2\,\Delta r/K_s}$$

$$(a_W + a_S)T(1,N) = a_W T(1,N-1) + a_S T(2,N) + b(1,N)$$

$$a_W = \frac{\Delta r}{2r_o\,\Delta\theta/K_e} \qquad a_S = \frac{r_s\,\Delta\theta}{2\,\Delta r/K_s} \quad (5)$$

On surfaces B and C, we have

$$(a_E + a_S + a_N)T(I,1) = a_E T(I,2) + a_N T(I-1,1) + a_S T(I+1,1) + b(I,1) \quad (6)$$

$$(a_W + a_S + a_N)T(I,N) = a_W T(I,N-1) + a_N T(I-1,N) + a_S T(I+1,N) + b(I,N) \quad (7)$$

Equations (6) and (7) are correct when $2 \le I \le M-1$; the coefficients a_E, a_N, a_S, a_W can be obtained using the method of Eq. (3) and were not written here.

If we apply the control-volume heat balance method to the control volume adjacent to the surface D, we obtain the following temperature equations on surface D.

$$[a_P + h(J)r_i\,\Delta\theta]T(M,J) = a_W T(M,J-1) + a_E T(M,J+1) + a_N T(M-1,J) + b(M,J) + h(J)r_i\,\Delta\theta T_f \quad (8)$$

where

$$a_E = \frac{\Delta r}{2r_i\,\Delta\theta/K_e} \qquad a_W = \frac{\Delta r}{2r_i\,\Delta\theta/K_w}$$

$$a_N = \frac{(r_i, 0.5\,\Delta r)\,\Delta\theta}{\Delta r/K_n} \qquad a_P = a_E + a_W + a_N$$

$$(2 \le J \le N-1)$$

Similar temperature expressions for $T(M,1)$ and $T(M,N)$ can be obtained as follows:

$$(a_P + 0.5h(1)r_i\,\Delta\theta)T(M,1) = a_E T(M,2) + a_N T(M-1,1) + b(M,1) + 0.5h(1)r_i\,\Delta\theta T_f \quad (9)$$

where

$$a_E = \frac{\Delta r}{2r_i\,\Delta\theta/K_e} \qquad a_N = \frac{(r_i + 0.5\,\Delta r)\,\Delta\theta}{2\Delta r/K_n}$$

$$a_P = a_E + a_N$$

$$(a_P + 0.5h(N)r_i\,\Delta\theta)T(M,N) = a_W T(M,N-1) + a_N T(M-1,N) + b(M,N) + 0.5h(N)r\,\Delta\theta T_f \quad (10)$$

where

$$a_W = \frac{\Delta r}{2r_i\,\Delta\theta/K_w} \qquad a_N = \frac{(r_i + 0.5\,\Delta r)\,\Delta\theta}{2\Delta r/K_n}$$

$$a_P = a_W + a_N$$

NONLINEAR HEAT SOURCE TREATMENT

So far, the algorithm expressions for $T(I,J)$ $(1 \le I \le M), 1 \le J \le N)$ have been obtained. After the nonlinear heat source term is determined, the above equations can be easily solved iteratively.

As sketched in Figure 2, we divide the half-tube into $M \times N$ grids. The total heat produced by the half tube per unit length is

$$Q = \bar{q}\pi r_i \quad (11)$$

On the other hand, the $M \times N$ parallel electrical resistances per unit length are assumed to operate at the same voltage V^*. The total heat produced by the $M \times N$ resistances is

$$Q = \frac{V^{*2}}{R_t} \quad (12)$$

where

$$R_t = \left(\sum_{I=1}^{M} \sum_{J=1}^{N} \frac{1}{R(I,J)} \right)^{-1} \qquad R(I,J)$$

is the electrical resistance of $P(I,J)$, and R_t is the total resistance of the $M \times N$ grids.

The heat created by control volume $P(I,J)$ per unit length is

$$b(I,J) = \frac{V^{*2}}{R(I,J)} \tag{13}$$

Combining Eqs. (11), (12), and (13), we obtain

$$b(I,J) = \frac{R_t}{R(I,J)} \bar{q} \pi r_i \tag{14}$$

where $R(I,J) = \rho(I,J)/A(I,J)$; $\rho(I,J)$ and $A(I,J)$ are the specific resistance and the cross-sectional area of control volume $P(I,J)$. For the stainless steel used in the present experiment, $\rho = 7.74 \times 10^{-7}$ $(1 + 7.45 \times 10^{-4} T)\ \Omega$ m, $K = 14.3(1 + 0.001T)$ W/(m °C).

INVERSE HEAT CONDUCTION PROBLEM SOLUTION (IHCS)

The inverse heat conduction problem is concerned mainly with the unknown boundary condition on the inner wall surface. This is subjected to a well-heat-insulated boundary condition at the outer radius. The discrete temperatures on the outer radius are assumed to be true values from measurements; the measurement error on the inner heat transfer coefficient is described in the next section.

In this problem, the number of unknown temperatures is $(M-1) \times N$ because $T(1,J)$ is known. Thus it is necessary to find $(M-1) \times N$ temperature solutions.

The heat-insulated boundary condition at surface A is used to obtain the temperature expressions for the second-layer nodes in the radial direction. This can be done by rewriting Eq. (3) into the following form:

$$T(2,J) = \big[(a_E + a_W + a_S)T(1,J) - a_E T(1,J+1) - a_W T(1,J-1) - b(1,J)\big]/a_S \tag{15}$$

For internal control volume $P(I,J)$, Eq. (2) is used to obtain the following temperatures:

$$T(I+1,J) = \big[a_P T(I,J) - a_E T(I,J+1) - a_W T(I,J-1) - a_N T(I-1,J) - b(I,J)\big]/a_S \tag{16}$$

Equation (16) is correct for $2 \le I \le M-1$ and $2 \le J \le N-1$.

When I is equal to $M-1$, we acquire the temperature expressions at the inner wall surface.

$$T(2,1) = \big[(a_E + a_S)T(1,1) - a_E T(1,2) - b(1,1)\big]/a_S \tag{17}$$

$$T(2,N) = \big[(a_W + a_S)T(1,N) - a_W T(1,N-1) - b(1,N)\big]/a_S \tag{18}$$

$$T(I+1,1) = \big[(a_E + a_N + a_S)T(I,1) - a_E T(I,2) - a_N T(I-1,1) - b(I,1)\big]/a_S \tag{19}$$

$$T(I+1,N) = \big[(a_W + a_N + a_S)T(I,N) - a_W T(I,N-1) - a_N T(I-1,N) - b(I,N)\big]/a_S \tag{20}$$

All temperature coefficients a_E, a_W, a_N, a_S, and $b(I,J)$, are calculated based on the method described for the direct heat conduction problem solution. Equations (15)–(20) constitute $(M-1) \times N$ unknown temperatures. These unknown variables can also be solved by the iterative method. After the temperature field is obtained, the local heat transfer coefficient and heat flux on the inner radius can be predicted.

For direct heat conduction problem solution (DHCS), the following iterative procedure is applied:

1. Specify the problem, including specifying tube dimensions, average heat flux, grid division, and a given inner heat transfer coefficient distribution.
2. Assume an initial tube temperature field.
3. Solve the algorithm equations $T(I,J)$, $1 \le I \le M$, $1 \le J \le N$. The iterative procedure is con-

tinued until $\|[T(I,J) - T^*(I,J)]/T(I,J)\| < \epsilon$; ϵ is set to be 10^{-6} in the present study.

For inverse heat conduction problem solution (IHCS), the iterative procedure is updated to the following:

1. Specify the problem, including specifying tube dimensions, average heat flux, grid division, and a given temperature distribution at the outer surface $T(1,J)$.
2. Assume an initial tube temperature field except for $T(1,J)$.
3. Solve the algorithm equations $T(I,J)$, $2 \le I \le M$, $1 \le J \le N$. The iterative procedure is continued until $\|[T(I,J) - T^*(I,J)]/T(I,J)\| < \epsilon$.

The heat transfer coefficients at the inner surface can be obtained from Eqs. (8)–(10); for instance, $h(J)(2 \le J \le N-1)$ is

$$h(J) = \frac{a_W T(M,J-1) + a_E T(M,J+1) + a_N T(M-1,J) - a_P T(M,J) + b(M,J)}{r_i \Delta\theta\left(T(M,J) - T_f\right)} \tag{21}$$

RESULTS AND DISCUSSION

Based on the methods introduced above, both a direct heat conduction problem code and an inverse heat conduction problem code are constructed. In order to verify the effectiveness of the inverse heat conduction solution, we did the comparative calculations using both codes for $r_o = 12.5$ mm, $r_i = 10.5$ mm, $T_f = 320.0$°C, $M = 20$, and $N = 10$. The grid numbers used were 20×10 with no obvious change in accuracy for the further increase of grid numbers.

Based on the experimental observations, just before the critical heat flux occurs, the temperature in the upper part of the tube may be much higher than that in the lower part of the tube, which induces the lower inner heat transfer coefficients in the upper part of the tube. In DHCS calculations, we assume a heat transfer coefficient distribution of $h(\theta) = 2{,}000 + 54{,}000(\theta/\pi)^2 - 36{,}000(\theta/\pi)^3$. With the above heat transfer coefficients, we obtained a lower heat transfer coefficient at top point $h|_{\theta=0} = 2{,}000$ W/m^2 °C) and a higher heat transfer coefficient at bottom point $h|_{\theta=\pi} = 20{,}000$ W/m^2 °C). The above heat transfer coefficient distribution is also even and continuous at $\theta = 0$ and $\theta = \pi$. The average inner heat flux is $\bar{q} = 200$ kW/m^2. At this condition, we obtained the temperature field using the DHCS solution: The discrete temperatures at the outer surface are predicted to be 401.74, 393.87, 377.44, 362.62, 352.83, 347.08, 343.76, 341.86, 340.84, and 340.51°C. The discrete temperatures on the outer radius obtained in DHCS solution are simulated as the true measured temperatures with zero mean temperature error, and treated as the input data in IHCS solution. With nonzero mean error, we added a normally distributed random error to each discrete temperature as 0.5, −0.3, 0.1, 0.4, −0.4, 0.3, 0.5, −0.4, 0.2, and −0.5°C. The IHCS solution acquired the inner heat transfer coefficients with zero mean error and nonzero mean error, and the heat transfer coefficients were compared with the assumed values in DHCS solution. The comparisons are shown in Table 1.

From Table 1, we know that the present inverse heat conduction solution is a useful tool in estimating the inner heat transfer coefficient. The comparisons between DHCS and IHCS solution with zero mean error show that the maximum relative error is only 0.95%. Generally speaking, larger error of estimated heat transfer coefficient may appear at $\theta = 0$ and $\theta = \pi$. The predicted temperature field by DHCS is very close to that by IHCS: We cannot even discern the differences between them. The predicted local heat flux is also very close to that by IHCS solution, and we found that $q(1) r_i \Delta\theta/2 + q(10) r_i \Delta\theta/2 + \sum_{J=2}^{9} q(J) r_i \Delta\theta$ is very close to $\bar{q}\pi r_i$, confirming the energy balance principle.

It should be noted that any temperature measurement includes errors. This leads us to perform sensitivity analysis of the temperature measurement error on the inner heat transfer coefficient. With nonzero mean error, the assumed maximum temperature error is 0.5°C and the maximum estimated heat transfer coefficient error is 8.0%. The estimated heat transfer coefficient errors decrease with decreasing temperature error at the outer radius, and also decrease with increasing temperature difference between the inside wall and the fluid. This is very useful in two-phase heat trans-

Table 1 Comparisons of heat transfer coefficients with zero and nonzero mean error

θ h (W/m^2 °C)	0	$\pi/9$	$2\pi/9$	$3\pi/9$	$4\pi/9$	$5\pi/9$	$6\pi/9$	$7\pi/9$	$8\pi/9$	π
DHCS solution	2,000	2,617	4,272	6,667	9,506	12,494	15,333	17,728	19,383	20,000
IHCS solution[a]	2,014	2,639	4,288	6,677	9,511	12,499	15,345	17,743	19,393	20,019
IHCS solution[b]	1,936	2,717	4,271	6,461	9,990	12,140	14,396	19,152	18,345	21,022
relative error %[a]	0.70	0.84	0.37	0.15	0.05	0.04	0.08	0.08	0.05	0.95
relative error %[b]	−3.20	5.00	−0.02	−3.10	5.10	−2.83	−6.10	8.00	−5.40	−5.11

[a]Zero mean error.
[b]Nonzero mean error.
The relative error is calculated as $(h_{\text{IHCS solution}} - h_{\text{DHCS}})/h_{\text{DHCS}}$.

fer experiment data analysis, especially in the critical heat flux region or the post-dryout region. Under such conditions, relatively larger temperature measurement errors at the outer radius produce only a little error on the inner heat transfer coefficient, due to the large temperature difference between the inside wall and the fluid.

Generally, the one-dimensional inverse heat conduction method requires fewer thermocouples to measure the temperature. However, for the present two-dimensional heat conduction problem, many locations are needed to obtain the temperatures at the outer surface due to the circular angle-dependent inner heat transfer coefficient. This can be easily done by welding the thermocouples on the outer surface.

Due to the need to develop a new, supercritical-pressure, once-through boiler in China, experiments with water at supercritical pressure flowing in inclined tubes were performed recently. The test tube, with dimensions of $\Phi 32 \times 3$ mm, was arranged at an inclined angle α of 14° or 10°. At a given cross section, seven thermocouples were welded at the outer surface of one half-tube. The maximum temperature error was estimated to be 0.5°C. The tube outer surface was also well heat insulated. With supercritical water flowing in inclined tubes, heat transfer shows special characteristics due to the complicated physical properties. A small change of fluid temperature can lead to large changes in heat transfer, especially in the near-pseudocritical region and the post-pseudocritical region. The heat transfer coefficient is lowest at $\theta = 0$ and highest at $\theta = \pi$, but the difference is small when the fluid temperature is much less than the pseudocritical temperature and it becomes larger in the near-pseudocritical and post-pseudocritical regions. For practical design interest, one wishes to know the heat transfer coefficient at $\theta = 0$. Typical examples are shown in Figure 4. The inner heat transfer coefficients at

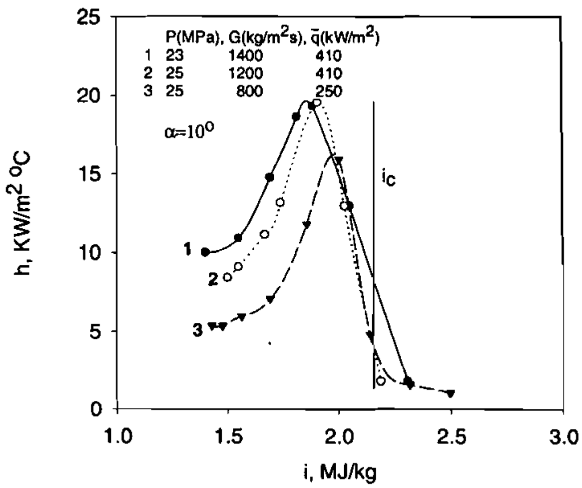

Figure 4 Heat transfer coefficients at $\theta = 0$ versus fluid enthalpy.

$\theta = 0$ are predicted using the present IHCS solution with the measured temperatures at the outer wall surface. The heat transfer coefficients attain maximum values just before the fluid reaches the pseudocritical temperature, then decrease sharply in the near-pseudocritical region (at the pseudocritical point, the specific capacity attains a maximum value). Such a phenomenon is similar to that with supercritical-pressure water flowing in vertical tubes, but the present experiment found that the heat transfer coefficients at $\theta = 0$ are nearly one-half of the heat transfer coefficients with supercritical-pressure water flowing in vertical tubes. Another example of wall temperatures, inner heat transfer coefficients versus circular angles, is shown in Figure 5 (post-pseudocritical region). Nonuniform heat transfer characteristics versus circular angles are detected in the near- or post-pseudocritical region even with high mass velocity flowing in the inclined tube.

The IHCS solution can be easily extended to some practical heat exchangers. However, the practical heat exchanger does not contain a heat-

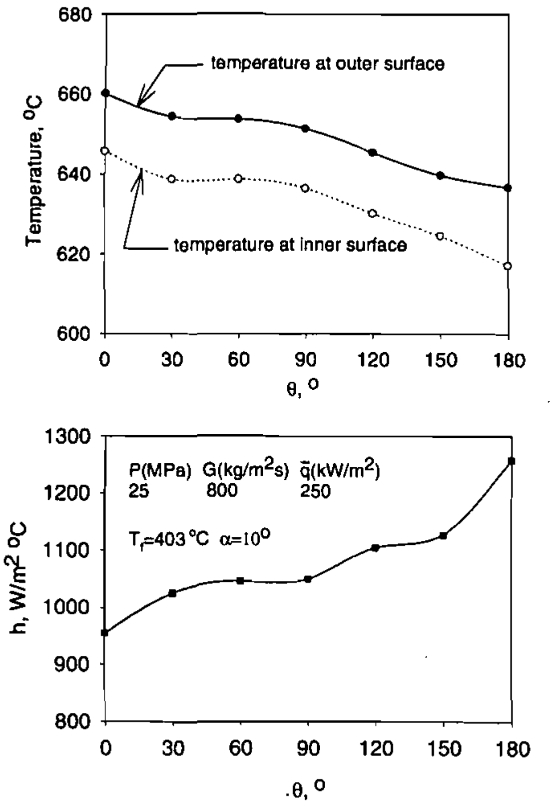

Figure 5 Temperature and heat transfer coefficients versus circular angle.

insulated boundary condition at the outer wall surface. An example is the heat exchanger used in chemical engineering. Such a heat exchanger uses high-temperature gas to heat the fluid from single-phase liquid to two-phase mixture with fluid flowing in horizontal tubes. The high-temperature gas may be stagnant or flowing, and the nonuniformly inner heat transfer coefficient at the cross section is due mainly to the two-phase mixture stratification. Usually the heat flux created by gas at the outer wall surface is uniform and can be given by the energy balance method, or the heat transfer coefficient at the outer wall surface can be estimated by some empirical correlations found in some classical literature. The control-volume energy equations adjacent to the outer wall surface should consider such heat flux. The wall temperatures at the outer wall surface should also be measured by thermocouples. In addition, the heat source term $b(I, J)$ in the IHCS solution is zero.

CONCLUSIONS

A steady-state, two-dimensional heat conduction model has been developed to calculate the temperature field. This is subjected to a given heat transfer coefficient angular profile on its inner radius and a well heat-insulated outer surface. The heat conductivity K and material specific resistance are considered as functions of temperatures. The nonlinear heat source term is considered by the concept of parallel electrical resistance heating. A nonlinear inverse heat conduction solution has also been constructed under the condition of well heat-insulated outer surface and the temperature measurement on the outer surface.

Comparative calculations were performed by both DHCS solution and IHCS solution with zero mean error and nonzero mean error. With increasing temperature difference between the inner wall surface and the fluid, the sensitivity of the noisy temperature measurement on the inner heat transfer coefficient is decreased.

The sensitivity of the noisy temperature measurement on the inner heat transfer coefficient is dependent on the thermocouples. Smaller-diameter thermocouple may produce small noisy error, thus higher accuracy of heat transfer coefficient may be obtained.

The advantage of the approach is that the solution is simple and needs little time to perform calculations.

NOMENCLATURE

a_E, a_W, a_N, a_S	temperature coefficients of east, west, north, and south surfaces, respectively
A	cross-sectional area of the control volume, m^2
b	heat produced by control volume per unit length, W/m
D_i	inside diameter of the tube, m
G	mass flow velocity, kg/m^2 s
h	heat transfer coefficient, W/m^2 °C
i	fluid enthalpy, J/kg
i_c	fluid enthalpy at pseudocritical temperature, J/kg
I	current flowing through the tube, A
K	thermal conductivity, W/m °C
L	length of the tube, m
M	total grid point in the r direction
N	total grid point in the θ direction
P	pressure, Pa or MPa
$\bar{q}$	average heat flux, W/m^2

Q	heat created by electrical resistance per unit length, W/m
r_i	tube inside diameter, m
r_o	tube outside diameter, m
r, θ	coordinates, Figure 2
R	electrical resistance per unit length, Ω/m
R_t	total electrical resistance of one half-tube per unit length, Ω/m
S	heat source term per volume, W/m^3
T	temperature, °C
T^*	last iterative temperature value, °C
T_f	fluid temperature, °C
V	voltage applied in the tube across a given tube distance, V
V^*	voltage per unit length, V
α	inclined angle with respect to horizontal direction, rad or deg
$\Delta r, \Delta\theta, \delta r, \delta\theta$	defined in Figure 2
ϵ	control variable
ρ	specific electrical resistance, Ω m

REFERENCES

[1] Beck, J. V., Blackwell, B., and St. Clair, C. R., Jr., *Inverse Heat Conduction*, John Wiley, New York, 1985.

[2] Hills, R. G., and Hensel, E. C., Jr., One-Dimensional Nonlinear Inverse Heat Conduction Technique, *Numer. Heat Transfer*, vol. 10, pp. 369–393, 1986.

[3] Flach, G. P., and Ozisik, M. N., An Adaptive Inverse Heat Conduction Method with Automatic Control, *J. Heat Transfer*, vol. 114, no. 5, pp. 5–13, 1992.

[4] Kurpisz, K., Numerical Solution of One Case of Inverse Heat Conduction Problems, *J. Heat Transfer*, vol. 113, pp. 280–286, 1991.

[5] Maillet, D., and Degiovanni, S., Inverse Heat Conduction Applied to Measurement of Heat Transfer Coefficient on a Cylinder, Comparison between an Analytical and a Boundary Element Technique, *J. Heat Transfer*, vol. 113, pp. 549–556, 1991.

[6] Keanini, R. G., and Desai, N. N., Inverse Finite Element Reduced Mesh Method for Predicting Multi-dimensional Phase Change Boundaries and Nonlinear Solid Phase Heat Transfer, *Int. J. Heat Mass Transfer*, vol. 39, no. 5, pp. 1039–1048, 1996.

[7] Patankar, S. V., *Numerical Heat Transfer and Fluid Flow*, Hemisphere, Washington, DC, 1980.

Jinliang Xu enrolled in Xian Jiaotong University in 1985, majoring in nuclear reactor engineering. He obtained master's and doctoral degrees at National Laboratory on Multiphase Flow of China in 1992 and 1995, respectively. His research interest is concentrated mainly in the field of two-phase flow and heat transfer. As a postdoctor, he is now undertaking a research project of probability safety analysis at Daya Bay nuclear power plant in China.

Tingkuan Chen obtained a master's degree in the Department of Thermal Engineering of Xian Jiaotong University in 1960. Since then he has been teaching and researching at Xian Jiaotong University. His research interest concerns the basic understanding of multiphase flow and heat transfer. He has also undertaken many projects in two-phase flow and heat transfer related to large-capacity boilers, nuclear power plants, and chemical engineering. Now he is one of the leaders of the National Laboratory on Multiphase Flow in Power Engineering of China.